

# Nanotube–Peptide Interactions on a Silicon Chip

Lifeng Zheng, Dheeraj Jain, and Peter Burke\*

Department of Electrical Engineering and Computer Science, University of California, Irvine, California 92697

Received: October 22, 2008; Revised Manuscript Received: December 22, 2008

Using the tools of modern molecular biology, we probe the interaction of nanotubes on silicon chips with proteins via combinatorial phage display methods. By screening against a large library of random peptides, we find that over half of the single-walled carbon nanotube (SWNT)-binding peptides show a motif of SXWXXW, where S is serine, W is tryptophan, and X is anything. In a helical wheel diagram, this peptide is amphiphilic, where the hydrophobic and aromatic tryptophan side groups are concentrated on one face of an  $\alpha$ -helix. This theme is robust and occurs in all of the SWNT-binding peptides. Surprisingly, the other aromatic amino acids seem less likely to show up in the screen, indicating a special role of tryptophan in binding to SWNTs. By elucidating the physical principles underlying the interaction between SWNTs and peptides and proteins, this work lays the foundation for the eventual human (or computer) nanoengineered, precise, and economical manipulation of nanotubes using peptides and proteins for nanotube sorting, assembly into electronic components, and understanding the effect of biological function.

## 1. Introduction

What is the nature of the interaction between carbon nanotubes and proteins? A reasonable working hypothesis is that certain peptides may bind with specificity to different nanotube allotropes (specific to the  $n$ ,  $m$  index). If this is true, then it may allow for economical peptide- and protein-based nanotube sorting and -purification technologies. Eventually, one may be able to engineer self-assembled, controllable placement and location control of nanotube devices with ( $n$ ,  $m$ ) precision using protein self-assembly analogous to so-called DNA nanotechnology. The development and understanding of nanotube interaction with living systems at the cellular level is also of significance for potential therapeutic and/or cytotoxic effects.<sup>1–3</sup> However, to date a thorough understanding of nanotube–protein interactions at the molecular level is still lacking, and the understanding of nanotube–peptide interactions can be considered the first and most fundamental step in understanding this complex system.

The hydrophobic nature of single-walled carbon nanotubes (SWNTs) is by now well known and prevents their solubility in aqueous solutions without the presence of surfactants. Thus, the study of surfactants<sup>4</sup> has been an important research theme and has led to a clear understanding that the nature of SWNT sidewalls can cause hydrophobic side groups of surfactants (anionic, cationic, and various surfactants) to bind noncovalently to SWNTs. DNA and some peptides also contain aromatic side groups that can bind to SWNTs via  $\pi$ – $\pi$  interactions, and thus act to solubilize SWNTs. As a biopolymer, peptides offer an astronomical variety of combinations of side groups and may allow us eventually to select on the basis of chirality and diameter. A recent precedent exists for diameter dependence and chirality dependence of SWNT–polymer binding (e.g., refs 5 and 6, reviewed in ref 7). Chirality-dependent binding by DNA was demonstrated by Zheng et al.<sup>8</sup> Diameter-dependent binding was demonstrated in early 2008 using a pentacene derivative by Tromp et al.<sup>9</sup> Whereas the ability of DNA to bind differently to semiconducting and metallic SWNTs has been demonstrated,<sup>10,11</sup>

the binding of proteins or peptides to nanotubes of differing electronic properties has not been demonstrated. Cyclic peptides with controllable pore diameter were found to bind to different-diameter tubes by Ortiz-Acevedo.<sup>12</sup> To date, no selectivity has been demonstrated for diameter, ( $n$ ,  $m$ ) index, or chirality based on linear peptides. Thus, there is much to learn about the interaction between SWNTs and peptides.

Because of the importance of aromaticity in SWNT binding, the three aromatic amino acids phenylalanine (Phe, F), tyrosine (Tyr, Y), and tryptophan (Trp, W) have been the focus of most studies to date. Dieckman et al. designed, synthesized, and demonstrated a SWNT binding amphiphilic  $\alpha$ -helix using Phe and Tyr (as well as artificial analog nitro-phenylalanine) side groups distributed along one face of the helix.<sup>13–15</sup> These peptides were found to disperse SWNTs effectively in solution.

Combinatorial phage display (PD), in which a combinatorial library of peptides expressed on the surface of a phage virus to screen for peptides with specific affinity for targets, has been applied to SWNTs in solution by Pender et al.<sup>16</sup> and Su et al.,<sup>17</sup> who found that His and Trp are important among SWNT-binding peptides. The role of Trp was further probed by Su et al.<sup>18</sup> using artificial analogs of Trp and studying their effect on binding to SWNTs. Wang et al.<sup>19</sup> studied binding to MWNTs using phage display techniques and found binding sequences that consisted of “symmetric surfactants”: hydrophilic on the ends and hydrophobic in the middle. In addition, His and Trp were found to play important roles, but not Phe. Using cell surface display<sup>20</sup> (rather than PD), Brown et al. found that His and also a large number of aromatic AAs are not required (only one is required) for binding to SWNTs on Si wafers. Very recently, Xie et al. studied the relative binding affinity of Trp, Phe, and Tyr to SWNTs using amino acids on the end of a surfactant peptide.<sup>21</sup> They found that Trp bound more strongly than Phe or Tyr. In summary, combinatorial screening techniques have demonstrated the importance of Trp in SWNT binding over the other two aromatic amino acids (Tyr, Phe), but the secondary structure was less significant. In contrast, a tailor designed secondary structure<sup>14</sup> (amphiphilic  $\alpha$ -helix) used the more weakly binding Phe side groups as the nanotube

\* Corresponding author. E-mail: pjburke@uci.edu.

“handles”. Our work, described next, combines the best of both of these approaches to find a new nanotube-binding peptide motif.

In this work, using a combinatorial phage display screen, we have experimentally discovered a nanotube-binding peptide that is qualitatively distinct from prior sequences determined using PD. We speculate that prior PD screening experiments did not find this binding sequence to be due to two key differences between our experiments and prior research. First, in our work, SWNTs are held in place on a Si chip during screening, whereas in prior experiments nanotubes were free-standing in the solution. This allows us to avoid the requirement of the use of surfactants to disperse nanotubes, which can interfere with peptide–nanotube binding during screening. Second, given this advance in experimental techniques, we have been able to develop a fundamentally new buffer appropriate to the hydrophobic nature of nanotube–peptide interaction. Prior research has used an acidic elution buffer to remove phages bound to SWNTs. An acidic elution buffer is most effective at disrupting electrostatic bonds. In nanotube interactions, noncovalent bonds are preferred if the pristine electronic and optical properties of nanotubes are to be preserved. Nanotube noncovalent binding moieties are known to be most effective if they are  $\pi$ – $\pi$ -type interactions. The new elution buffer that we have developed is more appropriate for disrupting these  $\pi$ – $\pi$  interactions and allows us to explore and discover the new nanotube-binding peptides described herein.

Our newly discovered structure consists of an  $\alpha$ -helix with Trp side groups distributed along one face of the helix. This allows the side groups to bind via  $\pi$ – $\pi$  stacking to the sidewalls of the nanotube using the strong interaction between Trp and SWNTs. This newly discovered peptide is remarkably similar to that designed from first principles by Dieckman et al.<sup>14</sup> using Phe and Tyr side groups but contains the much stronger nanotube-binding Trp side group instead. Thus, we make the first direct connection between rational, predictive SWNT-binding  $\alpha$ -helices and combinatorial screening for SWNT-binding peptides from a random library of random 12-mers. Given the recently developed understanding that Trp is a much stronger nanotube binder than Phe or Tyr, this new helix structure represents in some sense the most technologically advanced, naturally engineered nanotube-binding peptide developed to date.

## 2. Experimental Section

**2.1. Nanotube Synthesis.** SWNT samples were prepared by densely growing SWNTs on thermal oxide passivated silicon wafers. Thermal oxide silicon wafers were obtained by oxidizing p-type silicon wafers with crystal orientation (100) at over 1000 °C to an oxide film thickness of about 1  $\mu$ m. The silicon oxide wafers were then cut into 1 cm  $\times$  1 cm pieces with a dicing saw. After cleaning with acetone/methanol/DI water, some quartz and silicon oxide wafers were reserved as control samples. The others were dipped into a 1 mM FeCl<sub>3</sub> solution and rinsed with DI water, followed by drying with N<sub>2</sub> (g). These samples were then put into a 900 °C furnace with flowing methane and hydrogen to grow single-walled carbon nanotubes. (See ref 22 for growth details.) Representative SEM images of single-walled carbon nanotubes on silicon wafers are shown in Figure 1A.

**2.2. Nanotube Characteristics.** A variety of techniques exist to synthesize carbon nanotubes, which give rise to a variety of physical characteristics. In our technique, the nanotubes grow independently and do not cross until well into the growth phase.

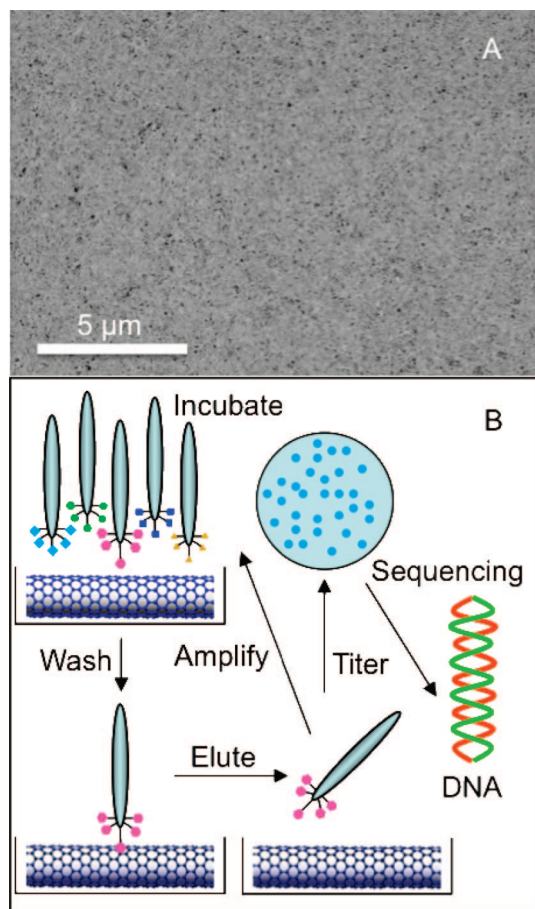


**Figure 1.** SEM images of SWNT networks on a SiO<sub>2</sub>/Si wafer (A) and the schematic phage display procedure (B).

Therefore, a reasonable assumption is that our nanotubes are individual, separated SWNTs, not ropes or bundles. One of the holy grails of SWNT synthesis is to be able to control and engineer the types of nanotubes that are synthesized. In our work, the diameter is controlled to be approximately 1.5 nm on average. However, the distribution of metallic vs semiconducting nanotubes is not controlled and is most likely a random distribution of (*n*, *m*) indices, which statistically predicts a ratio of metallic to semiconducting tubes of 1:2. Although it is well known that metallic and semiconducting nanotubes can have dramatically different kinetic reaction rates based on the different electronic densities of states, it is not known how noncovalent interactions such as  $\pi$ – $\pi$  bonding depend on the chirality. One of the long-term goals of our work is to use the knowledge gained from these studies to develop techniques to sort nanotubes on the basis of their (*n*, *m*) index. In summary, our nanotubes are individual SWNTs with an average diameter of 1.5 nm and a distribution of metallic and semiconducting species.

**2.3. Phage Display.** Phage display is a technique in which a random library of peptides is expressed on the surface of a phage virion.<sup>23</sup> The virions are allowed to incubate (bind) to a target (SWNTs in our case), whereas the unbound phages are washed away. The bound phages are eluted in a different buffer. The eluted phage contains sequences that bind to the target. To increase the specific selection, the cycle is typically repeated several rounds (9 to 10 rounds in our experiments), and then the phage DNA is sequenced to determine which peptide is expressed and hence has binding affinity for the target. The overall procedure is indicated in Figure 1B. In our experiments,

a random combinatorial library of 12-mer peptides (NEB Ph.D.-12 kit) expressed on the surface of the M13 phage was used.

**2.4. Titering and DNA Sequencing.** The eluted phage with the *lacZα* gene is exposed to and thus infects the *E. coli* ER2738 host strain ( $F^{\prime}$ -*recA*<sup>+</sup> $\Delta$ (*lacZ*)). The phage plaques are blue when plated onto LB/XGal/IPTG plates. The ratio of the total number of output phages after elution to the total number of input phages can be determined by titering the input and output eluate at each round (counting the numbers of blue plaques on the plates). Blue plaques were randomly picked for DNA sequencing to detect the motif of the binding peptides.

**2.5. Buffers.** There are four critical buffer solutions: blocking, incubation, wash, and elution buffers. Traditionally, blocking buffers are used to prevent the binding of the exposed substrates. Incubation buffers allow binding to occur. Wash buffers remove unbound phage, and elution buffers elute the bound phage for the next series of panning or sequencing. For traditional biological targets, a common blocking buffer solution is bovine serum albumin (BSA); TBS containing 0.1% v/v Tween-20 (TBST 0.1) is typically used for the incubation buffer. The Tween-20 detergent is supposed to separate phage particles from binding to each other. The wash buffer is typically TBST 0.1 for the first round, and the Tween-20 concentration is increased with each round stepwise by 0.1% to a final concentration of 0.5%. Here, Tween-20 prevents nonspecific binding (NSB) to the target and the substrate. The elution buffer is typically glycine-HCl with a pH of around 2. We have varied these buffer solutions to obtain optimal results. Because SWNTs (which are very hydrophobic) were the targets in our experiments, these traditional buffers were found not to be suitable. A different set of buffer solutions, appropriate to the nature of SWNT binding peptides, worked very well for carbon nanotube samples.

**2.6. Peptide Synthesis.** One of the peptides bound to the SWNT samples was synthesized using Fmoc techniques by a commercial vendor (ChemPep, Inc.) and purified to 97% for further analysis.

**2.7. CD Measurements.** Solutions of the synthesized peptide in DI water (100, 200, and 500  $\mu$ M) and TBS were prepared separately. CD measurements for these solutions were performed at room temperature using a 1 mm quartz cell on a Jasco J-810 instrument. Spectra were recorded over the range of 180–260 nm at a scanning speed of 2 nm/min.

**2.8. Dispersion Experiments.** SWNTs (1 mg, Cheap Tubes Inc.) was added to 1 mL of 100, 200, and 500  $\mu$ M solutions of the synthesized peptide in DI water or TBS. The mixtures were sonicated for 30 min to 1 h. After sonication, mixtures were centrifuged at 16 000g for 60 min. The visual appearance of the supernatant was used as a qualitative assessment of how well the SWNTs were dispersed by the peptides. A clear supernatant would indicate that most of the nanotubes were precipitated out and thus the peptide is not effective at dispersing the nanotubes, whereas a dark supernatant would indicate that the nanotubes were effectively dispersed by the peptide.

### 3. Results

In our experiments, we used SWNTs on silicon wafers grown in place via CVD using recipes as described in refs 22 and 24. A combinatorial library of peptides is expressed on the surface of a phage virus to screen for peptides with specific affinity for SWNTs, as shown in Figure 1. The nanotubes are strongly bound to but do not seamlessly cover the substrate, and hence a key challenge was to determine the peptide interaction with the substrate as opposed to the nanotubes. For this, the buffer selection was critical and is discussed next.

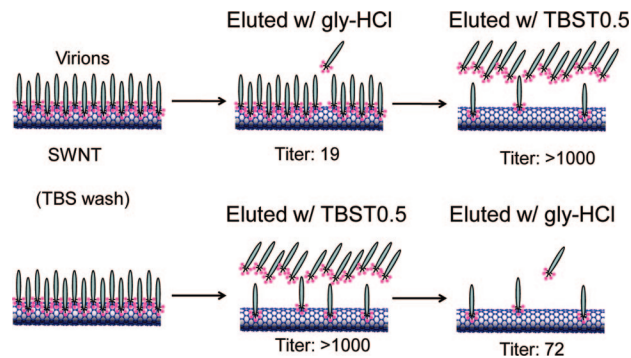


**Figure 2.** Titration results of 10  $\mu$ L 100 $\times$  dilutions of four eluants of samples A and B, after eluting twice with a different order of the two elution buffers. The washing solution was TBS.

**3.1. Elution Buffer: Dependence on the Peptide-Binding Mechanism.** In typical phage display experiments, acidic glycine-HCl is the most commonly used elution buffer.<sup>25</sup> Typically, the interaction between peptides and targets is an ionic interaction, and hence changing the solution pH is effectively expected to disrupt these interactions, allowing the effective elution of bound phages for further screening and amplification. However, as discussed above, the hydrophobic surfaces of nanotubes suggest that the nanotube-binding peptides may not bind via ionic bonds but rather through  $\pi$ - $\pi$  bonds. Thus, an acidic buffer may not be the most appropriate buffer for disrupting and eluting peptides that are bound to the surfaces of SWNTs.

We have conducted a set of experiments to analyze the efficiency of two different potential elution buffers. Two single-walled carbon nanotube (SWNT) samples A and B (SWNT CVD grown on  $1 \times 1$  cm<sup>2</sup> SiO<sub>2</sub> wafers) were both incubated for 45 min in TBS solution containing 4  $\mu$ L Ph.D-12 phage from the random library. Unbound phage was washed away with TBS five times. Sample A was first eluted with 0.2 M glycine-HCl (pH 2.2) and washed with TBS twice and then eluted with TBST 0.5. Sample B was first eluted with TBST 0.5 and washed with TBS twice and then eluted with glycine-HCl. All four eluants were titered. We found that TBST 0.5 eluted much more phage than glycine-HCl no matter what the elution order was, as indicated schematically in Figure 2. There might be a nontrivial fraction of phage eluted because of the nonspecific binding in the TBST eluants. Among the small number of phages eluted by glycine-HCl there might be quite a few phages eluted from the substrate because the surface of the SiO<sub>2</sub> wafers tends to be negatively charged and thus has a high affinity for positively charged peptides.

On the basis of the above results and analysis, we can conclude that TBST 0.5 is a better choice as an elution buffer for studying SWNT-peptide interactions. TBS can then be used as a washing buffer instead of TBST to avoid wash-off of the specific binders. However, the price of not using TBST as a washing buffer is that extra rounds of panning selection should be considered to remove the NSB phage. Further evidence to support this conclusion based on hydrophobicity measurements of the nanotube and control measurements is presented next.

**3.2. Wetting.** Whereas it is generally known that the surface of carbon nanotubes is hydrophobic, in our experiments this has given rise to some interesting observations that have not previously been reported. In Figure 3 below, we show a photograph of two SiO<sub>2</sub> wafers of the same size: one without nanotubes and the other with SWNTs. Whereas the bare SiO<sub>2</sub> wafer sinks, the hydrophobicity of the SWNTs is sufficient to



**Figure 3.** SWNT sample on a SiO<sub>2</sub> wafer suspended in water with the edge barely exposed to air while a SiO<sub>2</sub> wafer with no nanotubes sinks to the bottom of the glass container before half of its area is submerged in the water.

float the entire nanotube-coated wafer. More interestingly, when both of these samples are totally submerged in water, the SWNT sample can again float to the surface by swirling the container several times, but the bare SiO<sub>2</sub> wafer can not. This is a clear demonstration of the hydrophobicity of carbon nanotubes, even when on a SiO<sub>2</sub> surface. Measurements of water contact angles are consistent with this finding (Figure S2, Supporting Information). This can be used as a separate assay to measure the effectiveness of various elution buffers, discussed next.

During some of the biopanning experiments, we noticed that SWNT and control samples become fully wet (hydrophilic) after incubation in the phage solution. This is due to the binding of phage virions to the surface, which transformed the surface hydrophobicity. The surface became hydrophobic (for SWNT samples) and partially hydrophobic (for control samples) again after washing with TBST 0.1 followed by DI water, indicating that TBST was removing the phage virions. These phenomena of the hydrophobicity variation were not observed after samples were washed with TBS (no Tween-20) and eluted with glycine-HCl, indicating that glycine-HCl was not effectively eluting (removing) the phage virions. These observations clearly indicate (on a macroscopic scale) that Tween-20 is able to elute phage bound to nanotubes much more effectively than can the glycine-HCl buffer, consistent with the titering experiments discussed above.

**3.3. SWNT-Binding Peptide Motifs and Amino Acid Frequency Analysis: TBST Elution Buffer.** The goal of the experimental trials was to find a binding sequence that binds specifically to nanotubes (not the substrate). Convincing evidence for this would require two observations: First, the titer should gradually increase with increasing panning rounds. This would be due to the continual enrichment of nanotube-binding motifs in the pool of virions. Second, the control experiment (wafers with no nanotubes) should have a qualitatively different consensus motif of sequence than the nanotube sample.

A variety of buffers were used for washing and elution to achieve this goal, and we found that using TBST as the elution buffer allowed us to observe completely different motifs between nanotube-coated wafers and control wafers with no nanotubes. This elution buffer is different than in prior nanotube PD experiments. Sixteen of 19 sequences obtained from two SWNT samples were found to be very rich in tryptophan. The sequences are shown in Table 1. Among them, 11 sequences showed a motif of SXWXXXW.

The percentage of each amino acid in the random library is known. We have compiled data on the relative occurrence of

each amino acid in our peptides from the biopanning experiments, and the results are plotted in Figure 4.

Histidine is a very commonly occurring amino acid in the control experiments. We interpret this as a binding sequence to SiO<sub>2</sub>. The imidazole ring of histidine is partially protonated in aqueous solution (at neutral pH) whereas the SiO<sub>2</sub> surface is negatively charged. Hence, the interaction between the peptides and SiO<sub>2</sub> is likely electrostatic. This electrostatic mechanism also explains the nontrivial occurrence of positively charged lysine (K) shown in Figure 4.

However, there are only 4 occurrences of histidine in the 228 amino acids in the nanotube samples, which is only a quarter of the observed frequency in the NEB library. Histidine was found with enhanced probability in the pool of phage binding to the control sample containing no nanotubes, though, and is discussed in more detail below.

In contrast, the Trp-rich peptides occur in a high ratio for the nanotube samples. Besides the peptides with the SXW-WXXXW motif, those Trp-rich peptides without the motif are believed to bind to SWNTs as well via the  $\pi$ - $\pi$  interaction between the indole rings of Trp residues and the rings of SWNTs.

Thus, we conclude that the Trp-rich binding sequences are specific to nanotube binding because under this same set of buffer conditions the control sequences on wafers with no nanotubes were qualitatively distinct.

Why does the peptide sequence for SiO<sub>2</sub> not appear in the sequences for SWNTs on Si? Our hypothesis is that the nanotube-binding peptides are eluted with TBST much more efficiently than are the SiO<sub>2</sub> binding peptides. In the next set of results described, using glycine-HCl as the elution buffer, the peptide sequences for SiO<sub>2</sub> do appear in the samples coated with SWNTs, providing further evidence to support this hypothesis.

It is worth mentioning that a new peptide with the sequence SVSVGMKPSRP was observed. This peptide has no similarity to the ones binding either to SWNTs or to SiO<sub>2</sub> substrates. A literature search shows that peptides with this sequence can bind to human CSF antibodies,<sup>26</sup> mouse mAb 9-2-L379,<sup>27</sup> FePt,<sup>28</sup> and SiO<sub>2</sub> (0 0 1).<sup>29</sup>

**3.4. SWNT-Binding Peptide Motifs and Amino Acid Frequency Analysis: Glycine-HCl Elution Buffer.** In a separate series of experiments (Supporting Information, Figures S4–S8), we used 0.25 M glycine-HCl (pH 2.2) as the elution buffer instead of TBST. In these experiments, both the nanotube samples and the control wafers with no nanotubes had similar binding sequences. When the incubation and wash buffer were TBS, the sequences found were His-rich. We conclude that the motifs obtained in these experiments are the result of the interaction between peptides and SiO<sub>2</sub> substrates instead of SWNTs. This conclusion is also consistent with recent phage display work<sup>30</sup> on binding motifs to SiO<sub>2</sub>, which show that His-rich sequences bind preferentially to SiO<sub>2</sub>.

As discussed above, because histidine is protonated in aqueous solution (at neutral pH) and the SiO<sub>2</sub> surface is negatively charged, it is reasonable to infer that the interaction between the peptides and SiO<sub>2</sub> is electrostatic. In this case, an acidic elution buffer is expected to be more efficient at eluting SiO<sub>2</sub>-bound peptides, and this is indeed what is observed in these experiments.

We also found another motif for SiO<sub>2</sub> binding peptides when the incubation buffer was varied but the elution buffer was still glycine-HCl. We found a motif of RPXTG, again due to the interaction between a phage and SiO<sub>2</sub>. A similar motif (RP or

**TABLE 1: Sequences of Peptides Bound to Single-Walled Carbon Nanotubes**

no.	amino acids												occurrence
P1	D	D	W	S	H	W	W	R	A	W	N	G	3
P2	Y	T	S	P	W	W	L	A	W	Y	D	P	2
P3	A	W	W	E	A	F	I	P	N	S	I	T	1
P4	W	F	P	I	A	W	P	E	S	W	Y	H	1
P5	G	W	D	W	A	Q	D	W	N	W	W	T	1
P6	N	D	N	P	W	L	M	W	L	K	N	W	1
P7	Y	E	Y	P	W	A	N	W	W	L	S	P	1
P8	S	S	A	W	W	S	Y	W	P	P	V	A	6

PR) was observed in metal oxide binding peptides using cell-surface display techniques.<sup>31</sup> This further validates the conclusion that the binding motif determined using the glycine-HCl elution buffer was specific to the SiO<sub>2</sub> substrate and not the nanotubes.

We surmise that glycine-HCl does not elute phage particles specifically bound to nanotubes as efficiently as those bound to the SiO<sub>2</sub> substrate. This is consistent with wetting experiments described in the prior section. Thus, the peptides from these experiments were only SiO<sub>2</sub>-binding peptides, and this is why the nanotube-only samples did not show a unique motif.

**3.5. GES Scale Analysis.** Using the GES scale,<sup>32</sup> we have calculated the mean hydrophobicity for all of the clones from each experiment. The results of this analysis are presented in Figure 5 below. It is clear that in the experiment where specific binders to SWNTs were found the peptides are the most hydrophobic. This is consistent with the known hydrophobicity of SWNTs. However, as shown in Figure 6, in contrast to the work of Wang et al.,<sup>19</sup> most of our peptides are not symmetric surfactants, which we discuss below. We note that for the His-rich peptides found that bind to SiO<sub>2</sub> (when glycine-HCl was used as a buffer) the mean hydrophobicity (Supporting Information S8) was almost the same for the nanotube and control samples, again supporting the conclusion that the glycine-HCl eluted peptides were not nanotube binders.

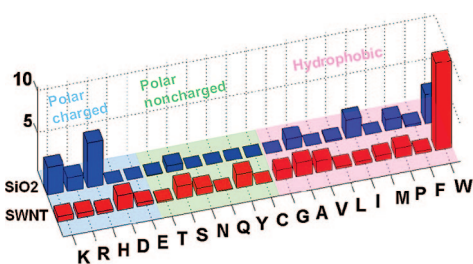


**Figure 4.** Relative occurrence of amino acids in nanotube and control experiments. The red and blue bars are for SWNT samples and their controls, respectively.

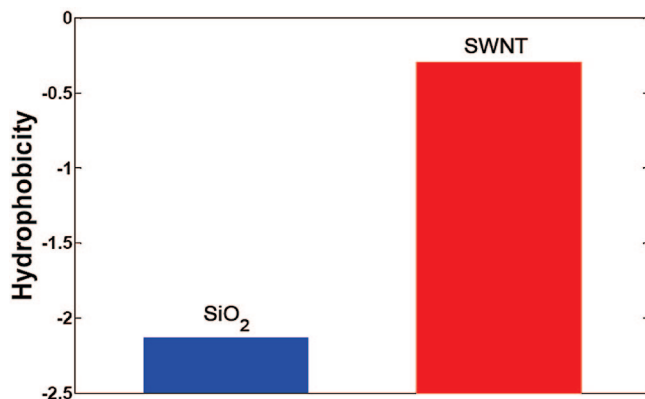


**Figure 5.** Mean hydrophobicity for nanotube and control binding peptides.

**3.6. CD Measurements.** One of the peptides bound to SWNTs on the Si substrates, P1 (DDWSHWWRWANG), was synthesized for CD measurement and nanotube dispersion. P1 was suspended in DI water only after sonication for 2 min, which demonstrates that P1 is fairly hydrophobic and thus is poorly suspended in water.

CD spectra of P1 were recorded for an aqueous solution and for a solution in TBS. The resultant spectrum was found to be independent of peptide concentration for the two concentrations studied, 100 and 200  $\mu$ M, whereas the spectra for a 500  $\mu$ M aqueous solution of peptide was slightly upshifted with noisy peaks. The spectrum (shown in Figure 7) indicates that the peptide is a random coil under the conditions studied.

**3.7. Nanotube Dispersion.** A small number of SWNTs were added to 1 mL of 100, 200, and 500  $\mu$ M aqueous solutions of P1, and the mixtures were sonicated for 30 min. The reason was to test with SWNTs that are free in solution, as others used previously. It was observed that even prolonged sonication did not help in dispersing the nanotube in solution. Black clumps

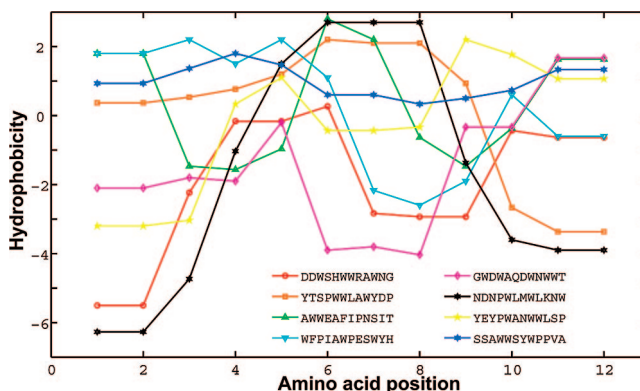


**Figure 6.** Amino acid hydrophobicity of nanotube-binding peptides using the GES scale.

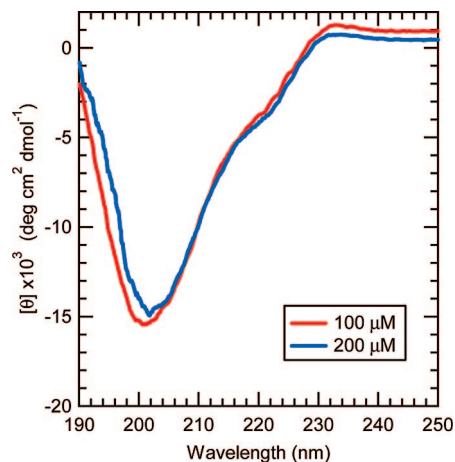


**Figure 7.** CD measurement of peptide P1 (DDWSHWWRWANG) in aqueous solution at two different concentrations.

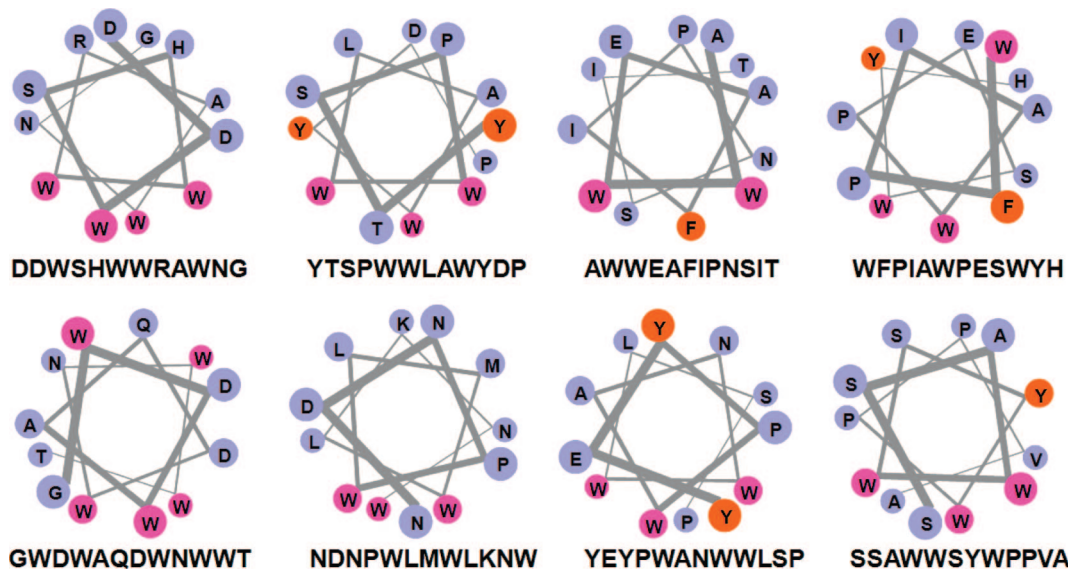


**Figure 8.** Helical wheel presentations of the peptides that are found that bind to SWNTs. Tryptophan residues (W) are highlighted in purple and consistently appear on one face of the helix.

formed in the solution, and the remaining solution was clear upon visible inspection. This is evidence that P1 is not effective at dispersing SWNTs in solution.

#### 4. Discussion

**4.1. Evidence for Binding to SWNT.** An important question is which binding sequences constitute SWNT-binding sequences as opposed to binding to other sites, such as the Si wafer or residual catalyst. Above we have already demonstrated that, with the appropriate buffer, we can discriminate between nanotube-binding and substrate-binding peptides. We now address the possibility of binding to the catalysts ( $\text{FeCl}_3$ ), which we do not believe is the case. First, the amount of catalyst is low because of the sample preparation process: the samples were rinsed with DI water after being dipped into the 1 mM catalyst solution. More importantly,  $\text{FeCl}_3$  is reduced to Fe and HCl during CVD growth. Fe is oxidized to  $\text{Fe}_2\text{O}_3$  after the growth. The specific binder to  $\text{Fe}_2\text{O}_3$  is known as RRTVKHHVN.<sup>33</sup> This binder contains mainly polar amino acids and should thus be hydrophilic, which is not shown in our results no matter if glycine-HCl or TBST was used as the elution buffer. As discussed above, one of the peptides that is found is known to bind to FePt, but this occurred only once. Thus, in summary, the binding of peptides to the catalyst seems to be unimportant in our experiments.

**4.2. Peptides Are Not Symmetric Surfactants.** The dispersion experiments indicated that P1 is not an effective surfactant because of its poor suspension. In prior PD work on MWNTs in solution, DuPont found that MWNT-binding peptides behaved as “symmetric surfactants” (i.e., the ends of the peptides were hydrophilic, and the central regions were hydrophobic). A quick inspection of Figure 6 shows that we find no such trend in our experiments. The reason that our experiments found different motifs is that we used a different elution buffer. In prior PD experiments, Tween-20 was used in both the incubation step and the washing step. Whereas Tween-20 in the washing step washed away the NSB phage, it also washed away the phage specifically binding to the carbon nanotubes via  $\pi$ – $\pi$  stacking. In fact, our results point to the conclusion that any surfactant would disrupt nanotube–peptide interactions and thus any PD measurement of free-standing nanotubes (which requires sur-

factant at all steps) would give rise to a qualitatively different set of nanotube-binding peptide motifs than that found in our experiments. A comparison of the literature to our experiments supports this claim. Thus, the best way to study peptide–nanotube interactions is with surface-bound SWNTs, where a surfactant is not required.

**4.3. Indication and Induction of an  $\alpha$ -Helix Structure.** In Figure 8, we show helical wheel presentations of all the peptides that bind to nanotubes. A helical wheel presentation assumes an  $\alpha$ -helix structure, which we have not directly proved. However, the results are striking. It is clear from this that the Trp residues are all located on one side of the helices. This general feature is included in all of the sequences found that bind to SWNTs. It seems highly unlikely that if the peptides are in a random coil distribution that all of the Trp residues would appear on one side of a helical wheel presentation. For example, if the peptides were randomly coiled, then Trp would be expected to show up with increased probability in the binding pool (which it did) because of its strong relative affinity for SWNTs but at random or semirandom locations along the peptide chain. The helical wheel presentation indicates the complete opposite (i.e., that Trp locations along the chain are far from random and consistently appear on one face of the helix, independent of the other amino acids in the chain).

However, our CD measurements of peptide P1 in solution indicated that it was not an  $\alpha$ -helix in solution but rather a random coil. We hypothesize that the peptides are random coils when in solution, except when they bind to the SWNTs on the Si wafers, and that the SWNT stabilizes and induces an  $\alpha$ -helix structure. We have not proven this hypothesis, but it is consistent with the data. It is well known that environmental effects play an important role in the conformational transition of peptides. Alteration in the temperature, pH, salt concentration, peptide concentration, and hydrophobicity of solution or redox state may switch peptides from one conformation ( $\alpha$ -helix,  $\beta$ -sheet, or random structure) to another.<sup>34</sup> A prior precedent appears in the work of Diekmann et al.,<sup>14</sup> where it was found that at 100  $\mu\text{M}$  concentration amphiphilic peptides are primarily a random coil (as determined via CD measurements) but when SWNTs were dispersed in the solution they induced the peptides to become  $\alpha$ -helices (again, as measured by CD). In our experi-

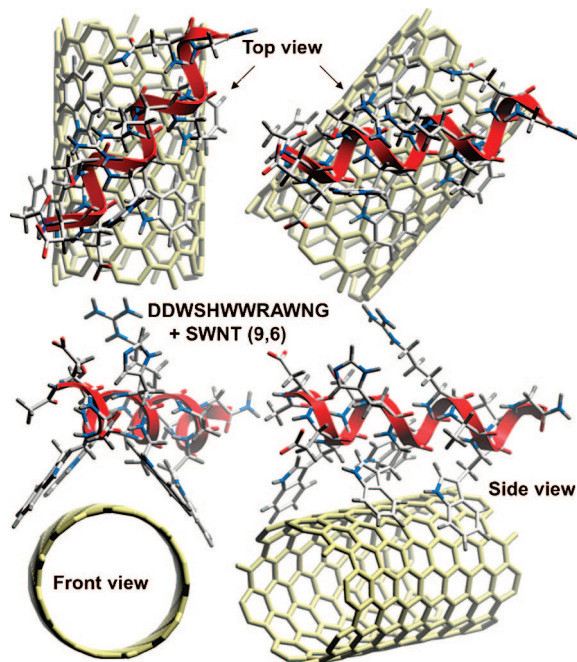


**Figure 9.** Nanotube–peptide docking (schematic).

ments, because the SWNTs were bound to the surface of a Si wafer, we were unable to perform CD measurements on the peptides when they were bound to the SWNTs to confirm this hypothesis. Such an experiment is beyond the scope of this article.

Thus, our conclusion is as follows: The peptides are random coils in solution and cannot support binding to SWNTs to solubilize/disperse them. Both CD and dispersion measurements support this claim. However, for SWNTs on Si wafers, the peptides adopt an  $\alpha$ -helix confirmation (which we infer), which allows the Trp residues to become aligned along one side of the helix, thus dramatically enhancing the binding to the SWNT sidewalls. Although the mechanism that induces the peptide to adopt an  $\alpha$ -helix confirmation at the SWNT/SiO<sub>2</sub> surface is not known, there are many similar examples of such peptide conformational changes induced by a surface or membrane. Although unexpected, this conclusion is the only scenario that consistently describes the ensemble of the experimental data presented in this article.

**4.4. Nanotube–Peptide Docking.** An accurate molecular model of the nanotube–peptide interaction is still under development.<sup>35</sup> However, it is generally believed that  $\pi$ – $\pi$  stacking is one mechanism for nanotube binding to aromatic side groups. With this in mind, we have manually investigated this possibility with our binding sequences, assuming that they form an  $\alpha$ -helix structure.

By manually rotating the torsion of the Trp side groups, we are able to generate a plausible geometry for nanotube–peptide docking. In Figure 9 (generated using the Molsoft ICM browser), we show an example of such nanotube–peptide binding geometry. We use peptide P1 (DDWSHWWRAWNG) with four Trp residues. These four residues are located between two planes with an angle of less than 90°. By slightly twisting the positions of the Trp residues, we can easily find that the peptide binds to a SWNT just like a clip clamping a rod (a SWNT (9, 6)) with about 1 nm diameter, as shown in Figure 9. Although this is not a true molecular dynamics simulation, it is a very plausible model for the nanotube–peptide binding geometry from our consensus sequences.

**4.5. Significance of Tryptophan.** Tryptophan is nonpolar and very hydrophobic amino acid with an indole functional group on the side chain, which can stack along the surface of carbon nanotubes. Thus, the appearance of tryptophan in our screen is no surprise. However, what is surprising is its appearance at a much higher frequency than that of the other aromatic amino acids, Phe and Tyr (Figure 4). Because Phe is a hydrophobic side group with aromatic content, it would reasonably be expected to occur in a nanotube-binding motif. In fact, a nanotube-binding peptide was also designed by Dieckmann et al.<sup>14</sup> using predominantly Phe residues. Thus, it appears that Trp has special significance in SWNT-binding peptides for reasons that we currently do not understand.

## 5. Conclusions

In this work, using a combinatorial phage display screen, we have experimentally discovered a nanotube-binding peptide that is qualitatively distinct from prior sequences determined using PD. The advance that allowed us to discover this new peptide was the development of a much improved elution buffer appropriate to the noncovalent interaction between nanotubes and peptides and the immobilization of nanotubes onto Si wafers during screening so that nonbinding nanotubes would not be lost during the experimental protocols (wash, incubate, centrifuge, etc.). Our newly discovered structure consists of an  $\alpha$ -helix with Trp side groups distributed along one face of the helix. This allows the side groups to bind via  $\pi$ – $\pi$  stacking to the sidewalls of the nanotube, using the strong interaction between Trp and SWNTs.

Because in our experiments we used a heterogeneous mixture of metallic and semiconducting nanotubes of varying diameter and (*n, m*) index, we have not been able to ascertain whether the nanotube-binding sequences are selective for different types. This is a clear goal for future research. Once we have developed a clear and quantitative understanding of nanotube–peptide interactions, we may ultimately be able to tailor design-specific protein structures to bind to nanotubes of a specific (*n, m*) index and use this process to manipulate, assemble, and possibly ultimately manufacture monodisperse, homogeneous nanotube devices and systems in an economical, large-scale fashion.

**Acknowledgment.** This work was supported by the Keck Foundation through a grant managed by the National Academy of Engineering Futures Initiative: Designing Nanostructures to Interface with Biological Systems.

**Supporting Information Available:** Protocol of phage display for the targets of SWNTs on chips and their control experiments; protocol of phage titering; protocol for the characterization of binding clones; water contact angles for the control wafer and SWNT-coated wafer; and titration results for SWNT and control samples after nine rounds of panning. This material is available free of charge via the Internet at <http://pubs.acs.org>.

## References and Notes

- (1) Paul, W.; Barone, M. S. S. Reversible Control of Carbon Nanotube Aggregation for a Glucose Affinity Sensor. *Angew. Chem., Intl. Ed.* **2006**, *45*, 8138–8141.
- (2) Yehia, H.; Draper, R.; Mikoryak, C.; Walker, E.; Bajaj, P.; Musselman, I.; Daigrepoint, M.; Dieckmann, G.; Pantano, P. Single-Walled Carbon Nanotube Interactions with HeLa cells. *J. Nanobiotechnol.* **2007**, *5*, 8.
- (3) Kam, N. W. S.; Liu, Z.; Dai, H. Carbon Nanotubes as Intracellular Transporters for Proteins and DNA: An Investigation of the Uptake Mechanism and Pathway. *Angew. Chem., Intl. Ed.* **2006**, *45*, 577–581.

- (4) Moore, V. C.; Strano, M. S.; Haroz, E. H.; Hauge, R. H.; Smalley, R. E.; Schmidt, J.; Talmon, Y. Individually Suspended Single-Walled Carbon Nanotubes in Various Surfactants. *Nano Lett.* **2003**, *3*, 1379–1382.
- (5) Chen, F.; Wang, B.; Chen, Y.; Li, L.-J. Toward the Extraction of Single Species of Single-Walled Carbon Nanotubes Using Fluorene-Based Polymers. *Nano Lett.* **2007**, *7*, 3013–3017.
- (6) Nish, A.; Hwang, J.; Doig, J.; Nicholas, R. Highly Selective Dispersion of Single-Walled Carbon Nanotubes Using Aromatic Polymers. *Nature* **2007**, *2*, 640–646.
- (7) Hersam, M. Progress Towards Monodisperse Single-Walled Carbon Nanotubes. *Nat. Nanotechnol.* **2008**, *3*, 387–394.
- (8) Zheng, M.; Semke, E. Enrichment of Single Chirality Carbon Nanotubes. *J. Am. Chem. Soc.* **2007**, *129*, 6084–6085.
- (9) Tromp, R. M.; Afzali, A.; Freitag, M.; Mitzi, D. B.; Chen, Z. Novel Strategy for Diameter-Selective Separation and Functionalization of Single-Wall Carbon Nanotubes. *Nano Lett.* **2008**, *8*, 469–472.
- (10) O'Connell, M. J.; Bachilo, S. M.; Huffman, C. B.; Moore, V. C.; Strano, M. S.; Haroz, E. H.; Rialon, K. L.; Boul, P. J.; Noon, W. H.; Kittrell, C.; Ma, J.; Hauge, R. H.; Weisman, R. B.; Smalley, R. E. Band Gap Fluorescence from Individual Single-Walled Carbon Nanotubes. *Science* **2002**, *297*, 593–596.
- (11) Zheng, M.; Jagota, A.; Semke, E. D.; Diner, B. A.; Mclean, R. S.; Lustig, S. R.; Richardson, R. E.; Tassi, N. G. DNA-Assisted Dispersion and Separation of Carbon Nanotubes. *Nat. Mater.* **2003**, *2*, 338–342.
- (12) Ortiz-Acevedo, A.; Xie, H.; Zorbas, V.; Sampson, W. M.; Dalton, A. B.; Baughman, R. H.; Draper, R. K.; Musselman, I. H.; Dieckmann, G. R. Diameter-Selective Solubilization of Single-Walled Carbon Nanotubes by Reversible Cyclic Peptides. *J. Am. Chem. Soc.* **2005**, *127*, 9512–9517.
- (13) Zorbas, V.; Smith, A. L.; Xie, H.; Ortiz-Acevedo, A.; Dalton, A. B.; Dieckmann, G. R.; Draper, R. K.; Baughman, R. H.; Musselman, I. H. Importance of Aromatic Content for Peptide/Single-Walled Carbon Nanotube Interactions. *J. Am. Chem. Soc.* **2005**, *127*, 12323–12328.
- (14) Dieckmann, G. R.; Dalton, A. B.; Johnson, P. A.; Razal, J.; Chen, J.; Giordano, G. M.; Munoz, E.; Musselman, I. H.; Baughman, R. H.; Draper, R. K. Controlled Assembly of Carbon Nanotubes by Designed Amphiphilic Peptide Helices. *J. Am. Chem. Soc.* **2003**, *125*, 1770–1777.
- (15) Poenitzsch, V. Z.; Winters, D. C.; Xie, H.; Dieckmann, G. R.; Dalton, A. B.; Musselman, I. H. Effect of Electron-Donating and Electron-Withdrawing Groups on Peptide/Single-Walled Carbon Nanotube Interactions. *J. Am. Chem. Soc.* **2007**, *129*, 14724–14732.
- (16) Pender, M. J.; Sowards, L. A.; Hartgerink, J. D.; Stone, M. O.; Naik, R. R. Peptide-Mediated Formation of Single-Wall Carbon Nanotube Composites. *Nano Lett.* **2006**, *6*, 40–44.
- (17) Su, Z.; Leung, T.; Honek, J. F. Conformational Selectivity of Peptides for Single-Walled Carbon Nanotubes. *J. Phys. Chem. B* **2006**, *110*, 23623–23627.
- (18) Su, Z.; Mui, K.; Daub, E.; Leung, T.; Honek, J. Single-Walled Carbon Nanotube Binding Peptides: Probing Tryptophan's Importance by Unnatural Amino Acid Substitution. *J. Phys. Chem. B* **2007**, *111*, 14411–14417.
- (19) Wang, S. Q.; Humphreys, E. S.; Chung, S. Y.; Delduco, D. F.; Lustig, S. R.; Wang, H.; Parker, K. N.; Rizzo, N. W.; Subramoney, S.; Chiang, Y. M.; Jagota, A. Peptides with Selective Affinity for Carbon Nanotubes. *Nat. Mater.* **2003**, *2*, 196–200.
- (20) Brown, S.; Jespersen, T. S.; Nygård, J. A Genetic Analysis of Carbon-Nanotube-Binding Proteins. *Small* **2008**, *4*, 416–420.
- (21) Xie, H.; Becraft, E. J.; Baughman, R. H.; Dalton, A. B.; Dieckmann, G. R. Ranking the Affinity of Aromatic Residues for Carbon Nanotubes by Using Designed Surfactant Peptides. *J. Pept. Sci.* **2008**, *14*, 139–151.
- (22) Li, S. D.; Yu, Z.; Rutherglen, C.; Burke, P. J. Electrical Properties of 0.4 cm Long Single-Walled Carbon Nanotubes. *Nano Lett.* **2004**, *4*, 2003–2007.
- (23) Baneyx, F.; Schwartz, D. T. Selection and Analysis of Solid-Binding Peptides. *Curr. Opin. Biotechnol.* **2007**, *18*, 312–317.
- (24) Yu, Z.; Li, S.; Burke, P. J. Synthesis of Aligned Arrays of Millimeter Long, Straight Single Walled Carbon Nanotubes. *Chem. Mater.* **2004**, *16*, 3414–3416.
- (25) Clackson, T.; Lowman, H. B. *Phage Display: A Practical Approach*; Oxford University Press: Oxford, U.K., 2004; pp xxiv, 332.
- (26) Manoutcharian, K.; Sotelo, J.; Garcia, E.; Cano, A.; Gevorkian, G. Characterization of Cerebrospinal Fluid Antibody Specificities in Neuro-cysticercosis Using Phage Display Peptide Library. *Clin. Immunol.* **1999**, *91*, 117–121.
- (27) Brett, P. J.; Tiwana, H.; Feavers, I. M.; Charalambous, B. M. Characterization of Oligopeptides That Cross-React with Carbohydrate-Specific Antibodies by Real Time Kinetics, In-Solution Competition Enzyme-Linked Immunosorbent Assay, And Immunological Analyses. *J. Biol. Chem.* **2002**, *277*, 20468–20476.
- (28) Reiss, B. D.; Mao, C. B.; Solis, D. J.; Ryan, K. S.; Thomson, T.; Belcher, A. M. Biological Routes to Metal Alloy Ferromagnetic Nanostructures. *Nano Lett.* **2004**, *4*, 1127–1132.
- (29) Tamerler, C.; Sarikaya, M. Molecular Biomimetics: Utilizing Nature's Molecular Ways in Practical Engineering. *Acta Biomater.* **2007**, *3*, 289–299.
- (30) Eteshola, E.; Brillson, L. J.; Lee, S. C. Selection and Characteristics of Peptides That Bind Thermally Grown Silicon Dioxide Films. *Biomol. Eng.* **2005**, *22*, 201–204.
- (31) Peelle, B. R.; Krauland, E. M.; Witttrup, K. D.; Belcher, A. M. Design Criteria for Engineering Inorganic Material-Specific Peptides. *Langmuir* **2005**, *21*, 6929–6933.
- (32) Engelman, D. M.; Steitz, T. A.; Goldman, A. Identifying Nonpolar Transbilayer Helices in Amino-Acid-Sequences of Membrane-Proteins. *Annu. Rev. Biophys. Biophys. Chem.* **1986**, *15*, 321–353.
- (33) Brown, S. Engineered Iron Oxide-Adhesion Mutants of the Escherichia coli Phage lambda Receptor. *Proc. Natl. Acad. Sci. U.S.A.* **1992**, *89*, 8651–8655.
- (34) Cerpa, R.; Cohen, F.; Kuntz, I. Conformational Switching in Designed Peptides: The Helix/Sheet Transition. *Folding Des.* **1996**, *1*, 91–101.
- (35) Tomasio, S. D.; Walsh, T. R. Atomistic Modelling of the Interaction between Peptides and Carbon Nanotubes. *Mol. Phys.* **2007**, *105*, 221–229.

## Supporting Information:

### Protocol of phage display for the targets of SWNTs on chips and their control experiments

#### Day 1

- 1 Inoculate 10 ml LB medium with ER2738 for titering. Incubate the culture at 37°C with vigorous shaking until  $OD_{600} = 0.5$  (mid-log phase).
- 2 Inoculate 25 ml LB medium with ER2738 for samples in a 250 ml Erlenmeyer flask. Incubate both cultures at 37°C with vigorous shaking until  $OD_{600} \sim 0.05-0.1$  (early-log phase).
- 3 Mix 1 ml of TBS and 10  $\mu$ l phage ( $4 \times 10^{10}$ ) from the NEB phage library in a well of a culture plate. Immerse the SWNT wafer in the phage solution. Rock gently, 45 minutes @ RT. Do the same to its control sample (the sentence is not repeated below).
- 4 Take out the SWNT wafer and wash it 5X, each time in a new well with 1 ml TBS.
- 5 Add 1 ml TBST 0.5 to a new well. Put the SWNT wafer into the well and rock gently for 45 minutes.
- 6 Take out the SWNT wafer and put it into a new well of a new plate and rinse with ddH<sub>2</sub>O 5 times. Pipet the eluate into a new microtube and label it.
- 7 Titer a small amount ( $\sim 10 \mu$ l) of the eluate. Follow the phage titering procedure. Usually 100X, 1000X,  $10^4$ X and  $10^5$ X for the unamplified eluate.
- 8 Add the rest of the eluate to the 10 ml early-log ER2738 culture in step 2. Incubate / vigorously shake @ 37 °C, 4.5 hours.
- 9 Pipet the culture into 8 microtubes, 1.25 ml each (only microcentrifuge is available in our lab). Spin 10 minutes @ 16,000 rpm / 4 °C. Transfer the supernatant to new microtubes and re-spin.
- 10 Pipet the upper 80% of the supernatant to the new microtubes and add 1/6 volume of PEG/NaCl. Allow phage to precipitate at 4°C overnight

#### Day 2

- 11 Do step 1 and 2. Count and record the blue plaques for the unamplified eluate.
- 12 Spin 8 microtubes of PEG precipitation, 15 minutes @ 16,000 rpm / 4 °C. Decant supernatant, re-spin briefly, and remove residual supernatant with a pipette.
- 13 Suspend the pellets together in 1 ml TBS. (*Here is how for 8 microtubes: suspend pellets of 4 of tubes each with 250  $\mu$ l TBS; transfer 250  $\mu$ l in the 4 tubes into another 4 tubes; mix the solution in the last tube.*)
- 14 Spin for 5 minutes at 4 °C to pellet residual cells.
- 15 Transfer the supernatant to a new microtube. Re-precipitate with 1/6 volume of PEG/NaCl. Incubate on ice 45 minutes. Spin 10 minutes @ 4 °C. Discard supernatant, re-spin briefly, and remove residual supernatant with a micropipet.

- 16 Suspend the pellet in 200  $\mu$ l TBS, 0.02% NaN<sub>3</sub>. Spin 1 minute to pellet any remaining insoluble matter. Transfer the supernatant to a new tube (*Note: This is the amplified eluate*). Label it.
  - 17 Titer a small amount ( $\sim 10 \mu$ l) of the eluate. Follow the phage titering procedure. Usually  $10^6$ X,  $10^7$ X,  $10^8$ X and  $10^9$ X for the unamplified eluate, depending on the titering results of the unamplified eluate. Count and record the blue plaques for the amplified eluate.
  - 18 Estimate the volume of the amplified eluate for  $10^{10}$  phages. It might need 100-150  $\mu$ l for the second round of panning. But the volume should be less for the subsequent rounds since more specific-binding phages are amplified.
  - 19 Mix that much volume of the amplified eluate with 1 ml TBS in a well of a new culture plate. Put the same SWNT sample into the well and rock gently for 45 minutes @ RT.
  - 20 Do steps 4-10.
- Day 3, 4, 5, ...
- 21 Do steps 11-20 until the motif of the sequences is achieved.

The general procedure is show in Figure S1.

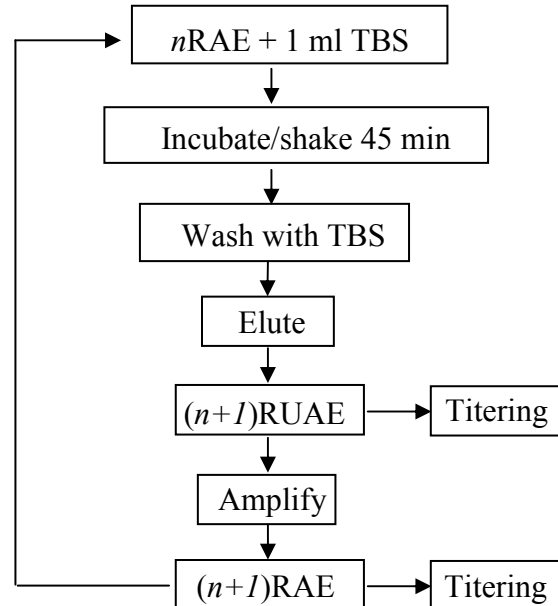


**Fig. S1.** The schematic process for phage display experiments. RT stands for Room Temperature;  $n$ R(U)AE for the  $n$ th-Round of (U)nAmplified Elution. 10  $\mu$ l NEB phage is used for 0RAE.

### **Protocol of phage titering**

- 1 Inoculate 5–10 ml of LB with ER2738; incubate with shaking until  $OD_{600} \sim 0.5$ .
- 2 Melt Agarose Top in microwave and dispense 3 ml into sterile culture tubes, one per expected phage dilution. Equilibrate tubes at 45 °C.
- 3 Pre-warm 1 LB/IPTG/Xgal plate per expected dilution at 37 °C.
- 4 Prepare 10-fold serial dilutions of phage in LB.
- 5 Dispense 200  $\mu$ l mid-log culture into microtubes, 1 for each phage dilution.
- 6 Add 10  $\mu$ l of each dilution to each tube, vortex quickly, and incubate at room temperature for 1–5 minutes.
- 7 Transfer the infected culture to a culture tube containing 45 °C Agarose Top, vortex quickly, and pour onto a LB/IPTG/Xgal plate. Swirling the plate to spread Agarose Top evenly.
- 8 Allow plates to cool 5 minutes, invert and incubate overnight at 37 °C.
- 9 Inspect plates and count plaques on plates having  $\sim 100$  plaques.

### **Protocol of characterization of binding clones**

- 1 Culture the ER2738 overnight ( $\sim 14$  hours) in a 250 ml Erlenmeyer flask and dilute 1:100 in LB. Dispense 1 ml diluted culture into each of 10 culture tubes.
- 2 Stab 10 blue plaques each with a new pipet tip and transfer them to the 10 culture tubes of step 1.
- 3 Incubate tubes at 37 °C with shaking for 4.5 hours.
- 4 Transfer cultures to microcentrifuge tubes, centrifuge 30 seconds. Transfer 500  $\mu$ l of the supernatant to a new microcentrifuge tube.
- 5 Add 200  $\mu$ l PEG/NaCl. Invert to mix, stand 10 minutes @ RT.
- 6 Centrifuge 10 minutes, discard supernatant. Re-spin briefly. Carefully pipet away any remaining supernatant.
- 7 Suspend pellet thoroughly in 100  $\mu$ l Iodide Buffer and add 250  $\mu$ l ethanol.
- 8 Incubate 10 minutes @ RT.
- 9 Spin 10 minutes, discard supernatant. Wash pellet in 70% ethanol, dry briefly under vacuum.
- 10 Suspend pellet in 30  $\mu$ l TE buffer.
- 11 Measure the density of ssDNA (ng/ $\mu$ l). Calculate the volume for 500 ng ssDNA.
- 12 Calculate the difference of 8 ml and the volume of ssDNA for ddH<sub>2</sub>O. Set 8 ml ssDNA and 0 for ddH<sub>2</sub>O if the volume of ssDNA is over 8 ml.
- 13 Mix the ssDNA and ddH<sub>2</sub>O in PCR strips.
- 14 Mail the PCR strips to Genewiz for sequencing.

**Fig. S2:** Water contact angles for control wafer and SWNT coated wafer.

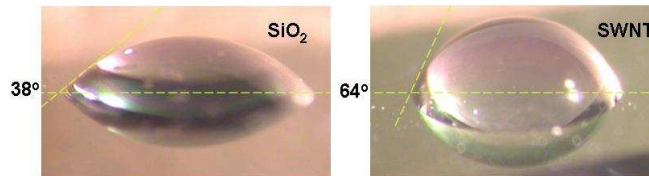


**Fig. S3:** Titration results for SWNT and control samples after 9-round panning.

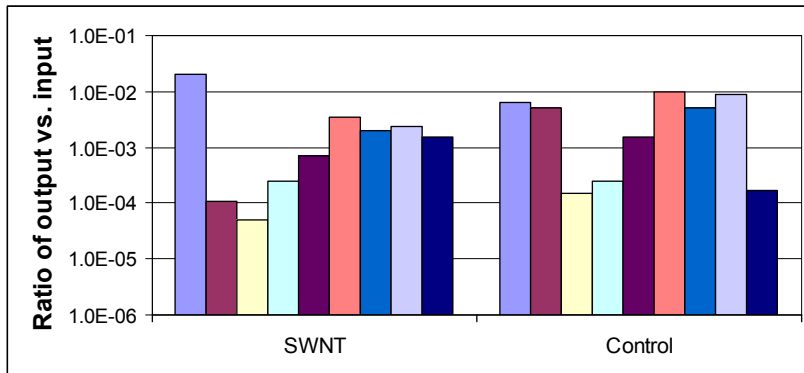


**Table S4.** List of experiments and buffer conditions used. Tween-20 concentration of TBST in wash buffer was increased stepwise by 0.1% from 0.1% to 0.5% v/v. S3 are the experiments with TBST elution buffer where a nanotube binding sequence was found (described in main text). The other experiments (Q1, Q2, S1, S2) used Glycine-HCl as the elution buffer, and found no difference between the nanotube and control samples, indicating the binding peptides were not binding to the nanotubes, but rather the substrates.

#	Target	Substrate	Blocking buffer	Incubation buffer	Wash buffer	Elution buffer	Motif
Q1	Nanotube	Quartz	BSA	TBST 0.1	TBST	Gly-HCl	H-rich
	Control	Quartz	BSA	TBST 0.1	TBST	Gly-HCl	H-rich
Q2	Nanotube	Quartz	---	TBST 0.1	water	Gly-HCl	H-rich
	Control	Quartz	---	TBST 0.1	water	Gly-HCl	---
S1	Nanotube	SiO2	---	TBST 0.1	TBST	Gly-HCl	RP
	Control	SiO2	---	TBST 0.1	TBST	Gly-HCl	RP
S2	Nanotube	SiO2	---	TBS	TBS	Gly-HCl	H-rich
	Control	SiO2	---	TBS	TBS	Gly-HCl	H-rich
S3	Nanotube	SiO2	---	TBS	TBS	TBST 0.5	W-rich
	Control	SiO2	---	TBS	TBS	TBST 0.5	H-rich

**Table S5.** Peptide sequences and their frequency of occurrence (F) of clones bound to nanotubes on quartz and control quartz wafers with no nanotubes.

Expt.	Peptide sequence											F	
Q1 SWNT on quartz	T	P	P	H	R	H	T	H	H	S	T	L	1
	K	P	P	H	S	H	K	H	P	L	L	T	1
	R	Y	Q	P	H	P	S	K	T	S	T	S	1
	H	I	M	P	H	L	I	P	V	S	V	L	1
	R	T	Q	S	Q	P	N	R	H	R	P	R	1
Q1 Control	A	P	A	H	L	H	K	P	S	H	V	R	1
	H	G	N	L	H	K	T	H	L	K	L	P	1
	K	Q	P	N	T	H	H	V	H	P	H	S	1
	S	P	K	W	H	P	H	H	Q	H	W	R	1
	H	L	R	T	H	P	S	H	H	N	V	P	1
	E	D	P	N	L	Q	S	S	L	R	M	P	1
Q2 SWNT on Quartz	H	L	T	P	T	S	T	W	S	N	P	H	2
	A	P	H	L	Q	H	G	H	H	P	H	R	1
	H	P	P	H	H	Q	T	H	H	R	T	P	1
	V	P	K	A	H	H	H	L	H	Y	E	A	1
	S	L	S	D	Y	H	R	S	P	Q	L	S	1
	N	P	G	N	Y	T	Q	Y	R	T	T	N	1

**Table S6:** Peptide sequences and their frequency of occurrence (F) of clones bound to nanotubes on silicon and control silicon wafers with no nanotubes.

Expt.	Peptide sequence												F	
S1 (SWNT)	P	R	P	A	L	S	T	G	P	G	R	F	2	
	R	P	L	Y	D	S	Y	N	T	G	M	R	1	
S1 (control)	P	R	P	A	L	S	T	G	P	G	R	F	1	
	P	S	N	K	R	R	K	D	L	A	N	V	1	
S2 (SWNT)	K	P	P	L	H	N	H	H	H	S	L	P	6	
	K	P	P	H	H	H	N	H	P	L	T	K	2	
	G	P	P	H	Y	H	K	H	K	L	S	A	1	
	L	P	H	H	G	H	T	H	K	M	R	V	1	
	H	K	L	Q	H	L	P	P	P	H	L	R	4	
	H	P	P	K	K	P	I	M	N	T	M	L	2	
	H	P	K	P	Q	H	A	H	L	K	P	V	1	
	H	G	T	K	P	P	H	L	H	S	V	R	1	
	H	K	Q	H	H	S	P	Q	N	F	S	L	1	
	K	P	P	D	R	H	V	H	K	L	P	I	1	
	S2 (control)	K	P	T	H	L	H	H	H	T	R	I	L	3
		K	P	L	H	V	H	R	H	H	V	M	D	1
K		P	V	H	P	H	Q	H	L	K	L	S	1	
K		P	I	H	H	H	P	H	L	P	L	K	1	
K		P	P	H	S	H	K	H	P	L	L	T	1	
I		P	P	H	P	H	A	H	H	Q	K	R	1	
A		P	K	N	H	V	H	H	V	H	K	S	1	
H		L	G	P	K	H	P	P	K	H	H	H	1	

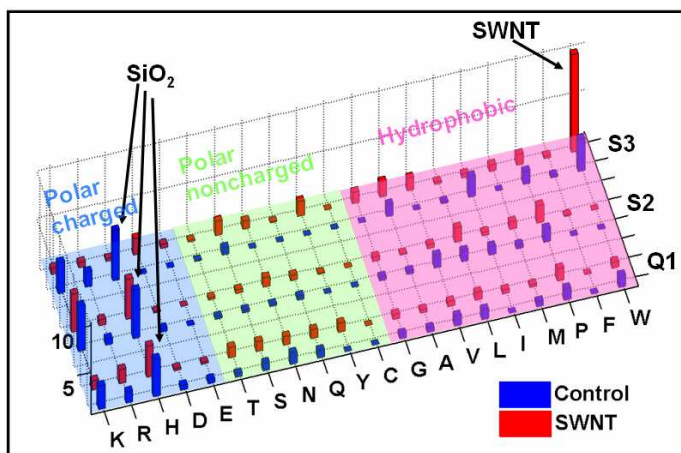


**Figure S7.** Relative occurrence of amino acids in nanotube and control experiments (Q1, S2 and S3). The red and blue bars are for SWNT samples and their controls, respectively.

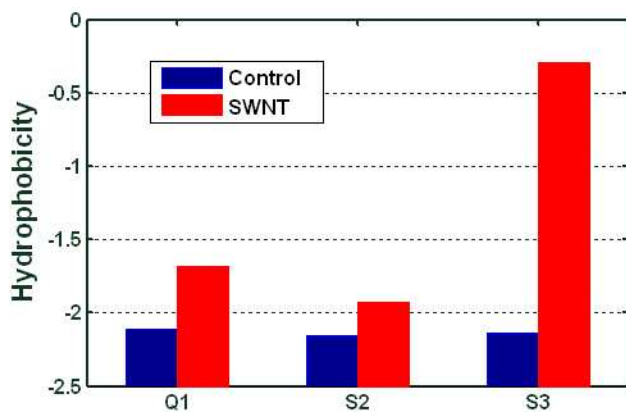


**Figure S8.** Average hydrophobicity for all peptides from each experiment.